Mechanical Heterogeneities in Model Polymer Glasses at Small Length Scales

Kenji Yoshimoto,[1] Tushar S. Jain,[1] Kevin Van Workum,[2] Paul F. Nealey,[1] and Juan J. de Pablo[1]

[1]*Department of Chemical and Biological Engineering, University of Wisconsin-Madison, Madison, Wisconsin 53706-1691, USA*
[2]*Polymers Division, National Institute of Standards Technology, 100 Bureau Drive, Stop 8542, Gaithersburg, Maryland 20899, USA*

(Received 30 April 2004; published 18 October 2004)

Molecular simulations of a model, deeply quenched polymeric glass show that the elastic moduli become strongly inhomogeneous at length scales comprising several tens of monomers; these calculations reveal a broad distribution of local moduli, with regions of negative moduli coexisting within a matrix of positive moduli. It is shown that local moduli have the same physical meaning as that traditionally ascribed to moduli obtained from direct measurements of local constitutive behaviors of macroscopic samples.

DOI: 10.1103/PhysRevLett.93.175501 PACS numbers: 62.20.Dc, 31.15.Qg, 62.25.+g

The elastic moduli of amorphous polymeric glasses have traditionally been characterized at length scales at which the material is treated as a mechanically homogeneous continuum [1]. Atomic-level studies of metallic glasses or polycrystalline materials have shown that such systems become spatially and mechanically heterogeneous at atomistic length scales [2–7]. In the particular case of glassy polymers, however, the length scale at which mechanical heterogeneities occur is not known. Interestingly, uses of polymeric materials in increasingly demanding nanofabrication applications require that an understanding of their mechanical behavior be developed at nanometer length scales [8].

In this Letter, we use molecular simulations to determine the local mechanical properties of glassy configurations of a polymer. The simulation cell is subdivided into small cubes of length l. By performing a microscopic momentum flux balance on a cube m, one arrives at the following expression for the local stress tensor, σ_{ij}^m [9,10]:

$$\sigma_{ij}^m = \rho^m k_B T \delta_{ij} - \frac{1}{l^3} \sum_{a<b} \left(\frac{\partial U}{\partial r^{ab}} \right) \frac{r_i^{ab} r_j^{ab}}{r^{ab}} \frac{q^{ab}}{r^{ab}}, \quad (1)$$

where ρ^m is the number density of cube m. Subscripts are used to denote Cartesian components. In the second term, U is a pairwise additive potential energy function and r^{ab} is the distance between two interaction sites a and b. If the vector joining a and b, denoted by r_i^{ab}, passes through cube m, the length of the line segment located inside cube m is defined by q^{ab}; otherwise, $q^{ab} = 0$. The term q^{ab}/r^{ab} determines how different pairwise interactions are apportioned to the local stress of cube m, and includes contributions from pairs of segments located outside the cube. Integration of σ_{ij}^m over the entire volume of the system yields the usual stress tensor of the bulk [11], denoted by σ_{ij} in what follows. Note that the local stress tensor shown in Eq. (1) is different from the so-called atomic-level stress tensor employed in previous studies of local moduli [2–4]. The latter is restricted to the stresses experienced by individual atoms, whereas the former is a spatial property of the system involving collective fluctuations of stresses acting on small domains.

For a system at equilibrium, the relation between the stress fluctuations and the local elastic modulus tensor, C_{ijkl}^m, is obtained from a second derivative of the free energy with respect to strain [7,9]:

$$C_{ijkl}^m = C_{ijkl}^{Bm} - C_{ijkl}^{Sm} + C_{ijkl}^{Km}, \quad (2)$$

where

$$C_{ijkl}^{Bm} = \frac{1}{l^3} \sum_{a<b} \left\langle \left(\frac{\partial^2 U}{\partial r^{ab2}} - \frac{1}{r^{ab}} \frac{\partial U}{\partial r^{ab}} \right) \frac{r_i^{ab} r_j^{ab} r_k^{ab} r_l^{ab}}{r^{ab2}} \frac{q^{ab}}{r^{ab}} \right\rangle, \quad (3)$$

$$C_{ijkl}^{Sm} = \frac{V}{k_B T} [\langle \sigma_{ij}^m \sigma_{kl} \rangle - \langle \sigma_{ij}^m \rangle \langle \sigma_{kl} \rangle], \quad (4)$$

$$C_{ijkl}^{Km} = 2 \langle \rho^m \rangle k_B T (\delta_{ik} \delta_{jl} + \delta_{il} \delta_{jk}), \quad (5)$$

and where V is the volume of the bulk system. The brackets denote a canonical ensemble average. The so-called Born term [12], C_{ijkl}^B, determines the instantaneous elastic modulus for any given configuration under a uniform, infinitesimally small strain. The use of the Born term alone is justified for affine or uniform deformation of all particles. Note, however, that the assumption of uniform displacement might not be justified at molecular length scales; the nonaffine or "internal" motion of particles gives rise to a decrease in the free energy after a homogeneous deformation [4,12–15]. This nonaffine component of the deformation has been shown to be particularly important in amorphous, two-dimensional systems [13]. In this Letter, the internal particle motion is driven by the thermal fluctuations, and is implicitly taken into account in our modulus calculation through the stress-fluctuation term, C_{ijkl}^{Sm} [15,16]. The contribution of the kinetic energy to the elastic modulus at each local domain is denoted by C_{ijkl}^{Km}. For amorphous polymers, we have found that the Born and the stress-fluctuation terms

are of comparable magnitude, and much larger than the kinetic term for all nontrivial components [17].

The polymer model considered in this work consists of 32 spherical interaction sites connected by harmonic springs. The nonbonded sites interact via a Lennard-Jones (LJ) potential energy function. In what follows, all quantities are reported in LJ reduced units [11]. The details of our model and of our sample preparation are outlined in Ref. [18]; long NPT molecular dynamics (MD) simulations were performed in which the temperature was gradually reduced from well above the glass transition temperature ($T_g = 0.43$). The number of chains and the pressure were fixed at 67 and 0.3, respectively. A glass configuration at $T = 0.10$ ($\rho = 1.05$) was used as a starting point for NVT MD simulations over 10^7 time steps ($\delta t = 0.001$). Ensemble-averaged local stresses, local densities, and local elastic moduli were calculated from Eqs. (1)–(5). A cubic simulation box of length $L(= 12.68)$ was subdivided into a grid of size $25 \times 25 \times 25$. The local elastic moduli at different length scales were calculated in cubic domains of length l ($2 \leq l \leq L$), centered at these grid points. All the results shown in this Letter were verified to be the same for configurations prepared from different initial states generated by Monte Carlo techniques [18] and long MD simulations.

Figure 1 shows local shear moduli profiles calculated for domains of different sizes. Because of limitations of space, results are only shown for the shear modulus, C_{1212}, which is simply denoted by G in what follows. By construction, at $l = L$, we obtain the volume-averaged elastic modulus corresponding to the modulus of the entire system. As l becomes smaller, the local shear moduli adopt a Gaussian distribution whose width increases progressively as the domain size is decreased. For the smallest domain size considered in this Letter, i.e., $l = 2$, approximately 8–10 monomers are contained in each domain. At $l = 2$, the stiff domains of the polymer can exhibit a modulus that is approximately three times as large as the average modulus of the system, whereas the soft regions can exhibit vanishingly small moduli. It is remarkable that these distributions remain Gaussian down to regions comprising only a few monomers. These findings should be contrasted with those of previous studies of elastic properties of amorphous metallic glasses. Such studies did not take into account contributions from stress fluctuations, and the reported distributions of G^m were non-Gaussian and always positive [3].

A noteworthy feature of the results shown in Fig. 1 is that some of the local shear moduli become negative. In general, a negative elastic modulus is indicative of a mechanically unstable material; a material that deforms spontaneously in the direction of an applied stress [4,19]. However, as shown in Fig. 2, the mechanical heterogeneities are not found to change over the course of long MD simulations; domains of strongly negative moduli remain negative. This finding suggests that the negative elastic moduli arise naturally in deeply quenched bulk amorphous polymeric glasses at molecular length scales. At

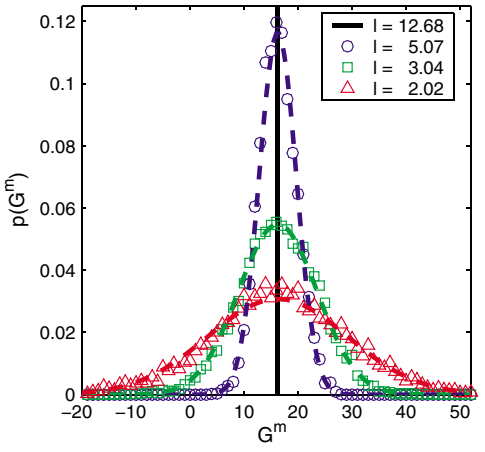

FIG. 1 (color online). Probability distribution function of local shear moduli, $p(G^m)$, for different domain sizes, l. The dotted lines correspond to Gaussian distributions characterized by the mean and standard deviation (SD) of data generated at each l. All the means are the same, 16.2, while the SDs depend on l; $SD = 3.4$, 7.3, and 13.0 for $l = 5$, 3, and 2, respectively. Note that all the nontrivial components of the elastic modulus tensor exhibit a behavior analogous to that of G^m. For instance, the local normal moduli (e.g. C^m_{1111}) are also characterized by Gaussians with mean 98.1 ± 1.2 and $SD = 37.4 \pm 4.1$ at $l = 2$.

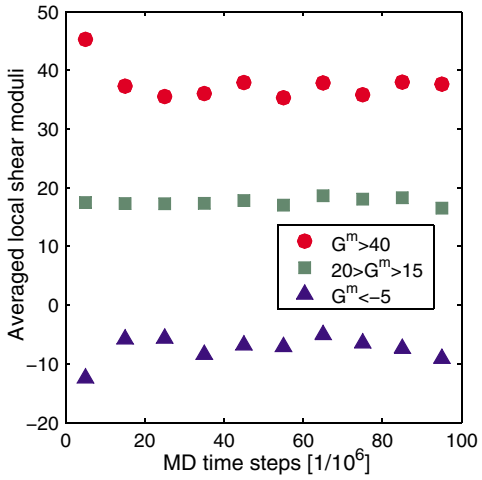

FIG. 2 (color online). Block-averaged local shear moduli for a long MD run. Local shear moduli were extracted from calculations for $l = 2$ (see Fig. 1), for domains of (△) strongly negative modulus, $G^m < -5$; (□) bulklike modulus, $15 < G^m < 20$; (○) strongly positive modulus, $G^m > 40$. Each block average corresponds to 10^7 MD time steps and each data point represents an average of the local shear moduli over the specified domains. Slight variations of strongly negative and positive moduli are a reflection of the thermal fluctuations of the local stresses.

higher temperatures (near or above T_g), the thermal motion of polymer segments becomes more significant, and as a result of ergodic restoring processes, the block-averaged local moduli approach the bulk mean value at that temperature over the length of the simulation.

In the following discussion, we concentrate our attention on the smallest length scales, namely $l = 2$. It is of interest to determine whether stiff or soft regions adopt specific spatial arrangements. Figure 3(a) shows that stiff regions coexist with much softer regions. To quantify this spatial inhomogeneity, the volume-averaged local shear modulus was calculated as a function of radial distance r around regions with either highly positive or negative elastic modulus [Fig. 3(b)]. For both types of region, the volume-averaged shear moduli approach the average at $r = 2$. In contrast, for regions that exhibit a shear modulus close to the average value, the volume-averaged local modulus does not exhibit significant variations with distance. These results show that domains of negative moduli are stabilized by surrounding regions of positive moduli, giving rise to a material that is stable over longer length scales. Recent experimental studies on macroscopic composite materials have shown that domains of negative stiffness can in fact be stabilized in a stiff matrix [19]. Such domains have also been observed at tilted grain boundaries in computer simulations of gold-copper bicrystals [4]. Our results, however, correspond to pure, completely amorphous polymeric materials and the reported heterogeneities arise at molecular-level length scales.

At macroscopic length scales, a shear modulus can be inferred from the linear relation, $\tau = G\gamma$. In order to determine whether the above relation holds at the smaller length scales considered in this Letter, a simple shear

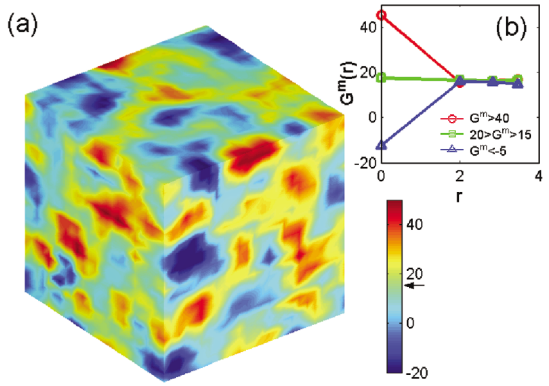

FIG. 3 (color). (a) Spatial heterogeneity of the local shear modulus at $l = 2$. The arrow in the scale bar indicates the bulk averaged shear modulus ($G = 16.2$). (b) Volume-averaged local shear modulus as a function of radial distance r. Different symbols indicate the nature of the region around which the average modulus was calculated; strongly negative ($G^m < -5$, triangles), bulklike ($15 < G^m < 20$, squares) or strongly positive ($G^m > 40$, circles).

deformation was applied to the system and the resulting change in the local stresses, $\tau^m (= \langle \sigma^m_{12,\gamma=0} \rangle - \langle \sigma^m_{12,\gamma>0} \rangle)$, was calculated. All the segmental positions were scaled initially by L and transformed into a deformed space with the so-called h matrix [20]. In MD simulations of 2×10^6 time steps, γ was increased in a stepwise manner by 5×10^{-4} in intervals of 10^4 time steps. The corresponding strain rate ($= 5 \times 10^{-5}$ in LJ units) was small enough [5,21] for the initial slope of the stress-strain curve to be in agreement with the modulus obtained from stress fluctuations [Fig. 4(a)]. In order to predict the change in local stresses, it was assumed that all domains are strained uniformly; $\tau^{mp} = G^m\gamma$. Figure 4(b) shows that cubes of strongly negative moduli (triangles) actually exhibit a decrease in stress as the shear strain is increased. In contrast, cubes having strongly positive moduli show a continuous increase of stress (circles), which is twice as large as that experienced by domains with bulklike moduli (squares).

An earlier study of a binary LJ glass former reported an inhomogeneous mechanical response at the atomic level [5]; after a plastic deformation, some of the changes of the atomic strain became negative (i.e. contrary to the direction of applied stress) or highly positive. It was speculated that atoms having abnormal shear moduli could be precursors of large corrective motion of atoms in plastic flow [2,5]. That negative strains occur at the

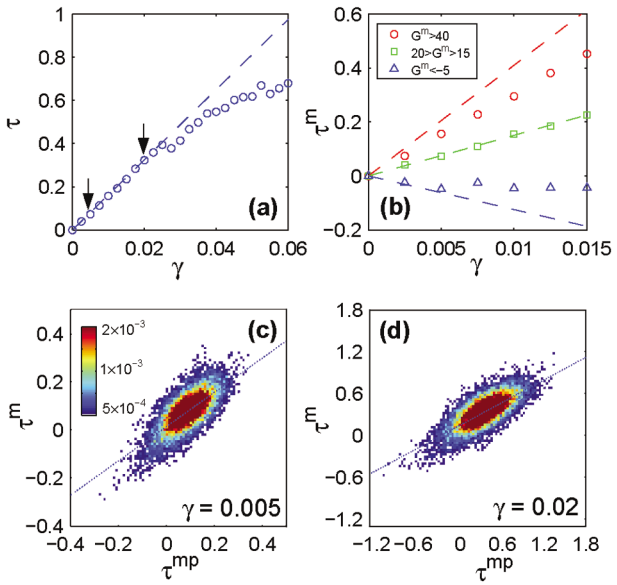

FIG. 4 (color). (Top row) Stress-strain relationship of (a) the entire system and (b) domains of strongly negative (△), bulklike (□), and strongly positive (○) moduli. The elastic response predicted from the shear modulus is shown by the dotted line. (Bottom row) Change in local shear stress τ^m versus predicted change in local stress τ^{mp} for all the domains at (c) $\gamma = 0.005$ and (d) $\gamma = 0.02$. The colors show the intensity of data at a given (τ^{mp}, τ^m). The dotted lines were obtained by a least-square fitting method.

atomic level is not particularly surprising. What is perhaps more intriguing is that for polymer glasses the negative moduli persist over relatively large regions of space comprising many particles.

In Fig. 4(b), strongly negative and positive moduli fail to predict τ^m for $\gamma > 0.0075$. We hypothesize that, for larger deformations, a discontinuity of τ^m occurs near the boundary regions of strongly negative and positive moduli and is relaxed by some local rearrangement of segments. In contrast, a large fraction of the local bulklike moduli still predict τ^m perfectly, anticipating the overall elastic response in Fig. 4(a). Note, however, that from $\gamma = 0.005$ to 0.02 (indicated by arrows in Fig. 4(a)], many of the bulklike domains with slightly larger (or smaller) moduli than that of the entire system also start to overpredict (or underpredict) τ^m; the long axis of the ellipse in Fig. 4(c) tilts clockwise in Fig. 4(d). Before $\gamma = 0.03$, the distribution of τ^m remains relatively narrow. At $\gamma = 0.03$, the spread of τ^m increases considerably and the deformation is accompanied by some large collective motions of segments; this is akin to the so-called local shear transformation observed in metallic glasses [5].

The concepts of local density and local stress are often invoked in discussions of material heterogeneities at interfaces, e.g., grain boundaries [4,6], free surfaces [22]. In the case of amorphous systems, it is intuitively appealing to expect a higher stiffness from a denser, more closely packed material. However, we have not found any significant correlations between the local shear modulus and the local density. Similarly, no strong correlation is observed between the local shear modulus and the local shear stress. In addition, we have not found significant correlations between the sign of the moduli and the motion of the particles in the corresponding domains during the simulation. This observation may be related to the conclusions drawn from the plastic deformation of atomistic polymer models [23,24].

Our finding of microscopic heterogeneities in the mechanical properties of glasses is of interest in light of recent experimental observations [25,26] related to the existence of dynamic heterogeneities in glasses, which are believed to arise at comparable length scales. The origin of dynamic heterogeneities is not well understood, but we expect them to be driven by heterogeneities of the stress. It would therefore be of interest to determine whether local mechanical properties are correlated or not with the rates of local molecular relaxation. As indicated above, the thermal motion of polymer molecules contributes significantly to the stiffness of a glass; we anticipate that the mechanical heterogeneities observed here will be decreased by free surfaces, where molecular mobility is greater than in the bulk [27,28], and that the spatial connectivity between domains of like moduli will be enlarged. This may become a crucial issue in the fabrication of nanoscopic polymeric glassy structures which is being pursued by the semiconductor industry [8,29].

We thank W. J. Drugan and J. F. Lutsko for discussions. This work was supported by Department of Energy, the National Science Foundation, and the Semiconductor Research Corporation.

[1] I. M. Ward, *Mechanical Properties of Polymers* (John Wiley & Sons, New York, 1971).
[2] K. Maeda and S. Takeuchi, Philos. Mag. A **44**, 643 (1981).
[3] T. Egami and D. Srolovitz, J. Phys. F. Met. Phys. **12**, 2141 (1982).
[4] I. Alber *et al.*, Philos. Trans. R. Soc. London A **339**, 555 (1992).
[5] D. Deng, A. S. Argon, and S. Yip, Philos. Trans. R. Soc. London A **329**, 613 (1989).
[6] M. D. Kluge, D. Wolf, J F. Lutsko, and S. R. Phillpot, J. Appl. Phys. **67**, 2370 (1990).
[7] K. Van Workum and J. J. de Pablo, Phys. Rev. E **67**, 031601 (2003).
[8] M. P. Stoykovich *et al.*, Adv. Mater. **15**, 1180 (2003).
[9] J. F. Lutsko, J. Appl. Phys. **64**, 1152 (1988).
[10] J. Cormier, J. M. Rickman, and T. J. Delph, J. Appl. Phys. **89**, 99 (2001).
[11] M. P. Allen and D. J. Tildesley, *Computer Simulation of Liquids* (Oxford University, New York, 1987).
[12] M. Born and K. Huang, *Dynamical Theory of Crystal Lattices* (Oxford University, New York, 1954).
[13] J. P. Wittmer, A. Tanguy, J. L. Barrat, and L. Lewis, Europhys. Lett. **57**, 423 (2002).
[14] J.W. Martin, J. Phys. C **8**, 2858 (1975).
[15] J. R. Ray, Comput. Phys. Rep. **8**, 109 (1988).
[16] S. Izumi and S. Sakai, JSME Int. J., Ser. A **47**, 54 (2004).
[17] K. Yoshimoto, Y. J. Papakonstantopoulos, J. F. Lutsko, and J. J. de Pablo (to be published).
[18] T. S. Jain and J. J. de Pablo, J. Chem. Phys. **120**, 9371 (2004).
[19] R. S. Lakes, T. Lee, A. Bersie, and Y. C. Wang, Nature (London) **410**, 565 (2001).
[20] M. Parrinello and A. Rahman, J. Chem. Phys. **76**, 2662 (1982).
[21] J. Rottler and M. O. Robbins, Phys. Rev. E **68**, 011507 (2003).
[22] F. Varnik, J. Baschnagel, and K. Binder, J. Chem. Phys. **113**, 4444 (2000).
[23] P. H. Mott, A. S. Argon, and U.W. Suter, Philos. Mag. A **67**, 931 (1993).
[24] F. M. Capaldi, M. C. Boyce, and G. C. Rutledge, Phys. Rev. Lett. **89**, 175505 (2002).
[25] H. Sillescu, J. Non-Cryst. Solids **243**, 81 (1999).
[26] M. D. Ediger, C. A. Angell, and S. R. Nagel, J. Phys. Chem. **100**, 13 200 (1996).
[27] J. A. Torres, P. F. Nealey, and J. J. de Pablo, Phys. Rev. Lett. **85**, 3221 (2000).
[28] K. C. Tseng, N. J. Turro, and C. J. Durning, Phys. Rev. E **61**, 1800 (2000).
[29] K. Van Workum and J. J. de Pablo, Nano Lett. **3**, 1405 (2003).